EPJ Web of Conferences **63**, 01018 (2013)
DOI: 10.1051/epjconf/ 20136301018

Development of a $LaBr_3$(Ce) Fast-timing Array for FAIR

O.J. Roberts[1,a], A.M. Bruce[1], Z. Patel[2], Zs. Podolyák[2], P.H. Regan[2,3], C.M. Townsley[2], A. Smith[4], K.F. Mulholland[5], and J.F. Smith[5]

[1] *School of Computing, Engineering and Mathematics, University of Brighton, Brighton, BN2 4GJ, U.K.*
[2] *Department of Physics, University of Surrey, Guildford, GU2 7XH, U.K.*
[3] *National Physical Laboratory, Teddington, TW11 0LW, U.K.*
[4] *University of Manchester, Oxford Road, Manchester, M13 9PL, U.K.*
[5] *Nuclear Physics Research Group, University of the West of Scotland, Paisley, PA1 2BE, U.K.*

Abstract. A γ-ray spectrometer with fast-timing capabilities, constructed of $LaBr_3$(Ce:5%) detectors, is under development for use at the future Facility for Anti-proton and Ion Research (FAIR). The physics aims of this device are to measure the half-lives of excited states in the region of ~50 ps to several ns, in exotic nuclei. Monte-Carlo simulations using the GEANT4 software package have determined the final design of this fast-timing array by calculating the full-energy peak efficiencies of several different detector geometries. The results of the simulated efficiencies for each configuration were used to calculate the timing precision. Consequently, an array of thirty six, ø3.8x5.1 cm cylindrical crystals was found to be the optimum configuration. The detectors were purchased and subsequently characterised, with each detector found to have intrinsic energy and timing resolutions of ~ 2.8 % (FWHM) and ~ 210 ps (FWHM) for the 1173 and 1332 keV decays from ^{60}Co.

1 Motivation

The development of a new Facility for Anti-proton and Ion Research (FAIR) [1] will include a new synchrotron and in-flight separator (Super-FRS) [2] capable of delivering a large number of high intensity, rare isotope beams. In order to exploit these beams, the Nuclear Structure, Astrophysics and Reactions international collaboration (NuSTAR), was established to develop and equip this new state-of-the-art facility with nine experimental setups. One such setup focuses on the DEcay SPECtroscopy of very short-lived nuclei at the extremes of existence [3, 4], where the combination of a high primary beam intensity and the Super-FRS will allow nuclei along the r-process path in neutron-rich nuclei to be studied. It is planned that a high-efficiency γ-ray spectrometer of $LaBr_3$(Ce) crystals will be used in a 'stopped beam' setup to measure half-lives of excited states in the region of 50 ps to 10 ns by taking the time difference between the γ rays feeding and de-exciting the level of interest using $\gamma\gamma$ coincidences [5]. This modular fast-timing array will work alongside charged particle [6] and (in cases with β-delayed emission of neutrons [7]), neutron detector arrays [8].

2 The Simulated Efficiency

In order to fulfil its use as an efficient spectrometer, the fast-timing array needs to subtend as much of the solid angle as possible with a crystal depth that is capable of detecting γ-ray photons up to ~4 MeV (the energy expected to be emitted by magic or semi-magic nuclei e.g. [9]), with reasonable efficiency.

Cylindrical crystals with dimensions; ø2.5x2.5 cm, ø3.8x3.8 cm, ø3.8x5.1 cm and ø5.1x5.1 cm were considered and compared with the 'hybrid' and conical crystals, two novel geometrical designs that have been shown to reduce the time spread associated with the scintillation collection process [10]. The 'hybrid' detector is defined as a truncated cone attached to a ø3.8 cm cylinder, with a total length of 4.7 cm. The conical crystals have front and back window diameters of 2.5 and 3.8 cm respectively, and a length of 3.8 cm.

The array will be used alongside the Advanced Implantation Detector Array (AIDA) [6] to make implant-decay correlations. AIDA consists of a stack of 20, 8x8 cm double-sided silicon strip detectors (DSSDs), of 0.1 cm thickness with 0.1 cm between each detector. Monte-Carlo simulations using the simulation package GEANT4 [11], were used to determine the full-energy peak (FEP) efficiencies of the fast-timing array and treated the AIDA implantation point (the centre of the 10^{th} DSSD), as a point source which emitted 10^6 γ-ray events with energies from 100 to 4000 keV. The aluminium can of AIDA, which has dimensions of 10x10x50 cm and thickness of 0.2 cm, was also included. The minimum radius for which an integer number of each detector type could be tiled in a ring around AIDA [6] was calculated to be 8.3 cm. The number of each detector type needed in one ring around

[a] e-mail: O.J.Roberts@brighton.ac.uk

Article available at http://www.epj-conferences.org or http://dx.doi.org/10.1051/epjconf/20136301018

Table 1. Details of the crystal types used in the simulations along with their timing resolution. The second row gives an estimated timing resolution for the ø3.8x5.1 cm crystal based on the interpolation of the known timing resolutions of the ø5.1x5.1 cm and ø3.8x3.8 cm detectors. The third row lists the measured timing resolutions from this work. The coincidence timing precisions (TP) were normalised to the ø2.5x2.5 cm detectors (see text for details).

#	Dimensions	T_{FWHM} (ps) at 511 keV	T_{FWHM} (ps) at 1332 keV	*Relative TP* at 511 keV	*Relative TP* at 1332 keV
8	ø5.1x5.1 cm	450 [12]	300 [5]	0.53	0.34
10	ø3.8x5.1 cm (estimated)	405	240	0.65	0.39
10	ø3.8x5.1 cm (measured)	400	210	0.64	0.34
10	ø3.8x3.8 cm	360 [12]	180 [5]	0.74	0.41
13	ø2.5x2.5 cm	200 [13]	150 [5, 14, 15]	1.00	1.00
13	ø2.5x3.8xø3.8 cm (conical)	-	160 [15]	-	0.44
13	ø1.9x4.7xø3.8 cm ('hybrid')	-	-	-	-

AIDA is presented in column one of Table 1, along with their typical timing resolutions at full-width half maximum (FWHM) in the middle two columns.

2.1 Timing Precisions

The FEP efficiencies for one ring of each of the proposed detector types were simulated, and the ring of 13 'hybrid' crystals was found to have the highest efficiency for $E_\gamma \geq 200$ keV. The ø5.1x5.1 cm crystals when tiled around the implantation point have more dead space between each detector than the 'hybrid' detectors due to the lack of truncation at the front of the crystals, resulting in a lower efficiency for $E_\gamma \geq 200$ keV. For $E_\gamma \leq 200$ keV, the 'hybrid' crystals have an efficiency comparable to that of the ø3.8x5.1 cm crystals due to the small diameter at the front of each crystal. A ring of eight ø3.8x5.1 cm crystals has the third highest FEP efficiency (~5 % for E_γ=500 keV). The FEP efficiencies of the ø2.5x2.5 cm and conical crystals were lower than the other simulated configurations.

The precision of a half-life measurement depends on the level of statistics and the timing resolution of the setup. A coincidence timing precision can be calculated using the efficiency and timing response of coincident detectors, defined to be the timing response (FWHM) divided by the square root of the total number of counts in the time peak [16].

The coincidence timing precisions are shown in the last two columns of Table 1 and were calculated using the timing resolutions shown in the same table for 511 and 1332 keV γ-rays, along with the simulated FEP efficiencies of a ring of each detector type. At this stage, the timing resolutions of the ø3.8x5.1 cm detectors were interpolated from the known timing resolutions of the ø3.8x3.8 cm and ø5.1x5.1 cm detectors. The largest crystals (ø5.1x5.1 cm and ø3.8x5.1 cm) were found to have a timing precision a factor of two and three times better than the ø2.5x2.5 cm crystals at energies of 511 and 1332 keV respectively. However the ø3.8x5.1 cm crystals were preferred in order to maintain the required need of a modular array. The coincidence timing precision for the 'hybrid' crystals was not calculated as no timing information for these detectors is available in literature. However, the timing resolution a 'hybrid' crystal must have in order for a ring of these crystals to have the same precision as a ring of ø3.8x5.1 cm cylindrical crystals in coincidence mode was calculated. For γ-ray energies of 511 and 1332 keV this was found to be 910 and 660 ps respectively. The ø3.8x5.1 cm and 'hybrid' crystals were therefore selected to be tiled into various full array configurations.

2.2 The Full Array Configuration

Two detector configurations around the AIDA implantation point were simulated; a cross configuration with additional crystals at 45° and a 'ball' setup. Multiplicity one γ-rays with energies up to 4 MeV were simulated in order to determine the FEP efficiencies. The left panel of Figure 1 shows that for both configurations, the 'hybrid' detector array has a higher FEP efficiency than an array of ø3.8x5.1 cm cylindrical crystals. When the 'hybrid' crystals are tiled into an array they cover more of the solid angle and are closer to the implantation point than the ø3.8x5.1 cm crystals, due to the tapering of the front of the crystals. However, the intrinsic energy and timing resolutions of this novel detector have not yet been sufficiently well characterised in order to make an informed decision. Therefore, the ø3.8x5.1 cm cylindrical crystals were chosen and are shown in a cross configuration with additional crystals at 45° in the right panel of Figure 1.

3 Characterisation of the $LaBr_3$(Ce) detectors

The results of the simulations and calculations from the previous sections resulted in the decision to purchase the ø3.8x5.1 cm detectors. Thirty one, ø3.8x5.1 cm $LaBr_3$(Ce) detectors were bought and characterised. Each crystal was coupled to a modified H10570 Hamamatsu PMT with optical grease from Midland Silicones Ltd. (MS 200, viscosity 10000). The energy signal was taken from the last dynode of the 8 stage PMT. The signals were found to be very fast and therefore the output impedance on the last dynode had to be changed from 51 Ω to 1000 Ω on all the PMTs, effectively increasing their integration times. This allowed the signals to be processed more effectively with analogue electronics. From the last dynode, the energy signal was then sent to a multi-channel analyser (ORTEC

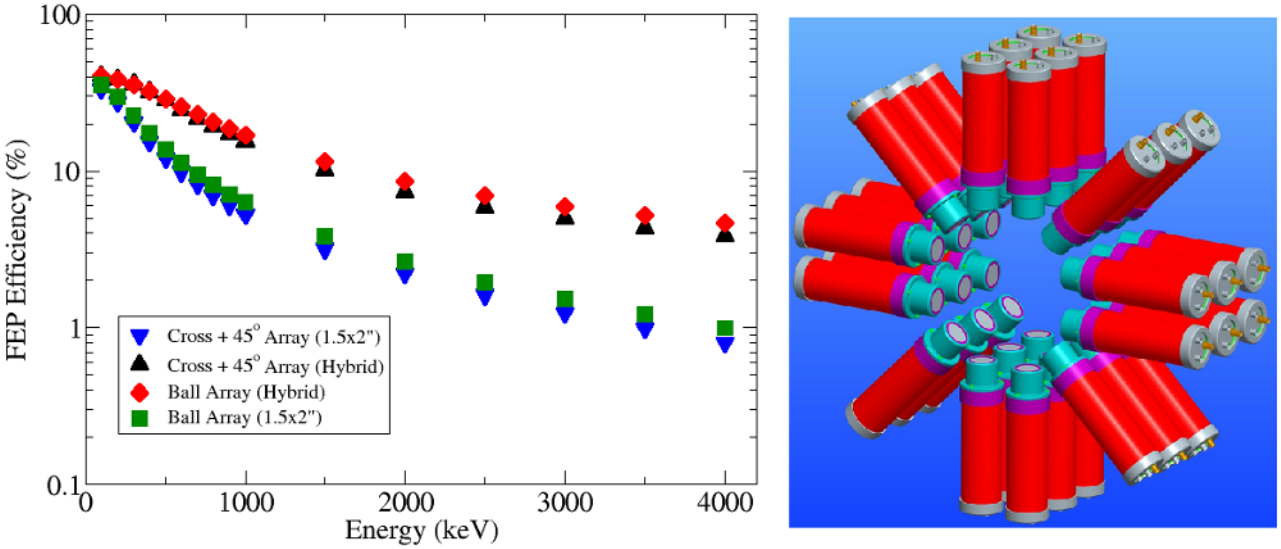

Figure 1. Left panel (Colour on-line): The FEP efficiencies of the 'hybrid' and ø3.8x5.1 cm crystals in different configurations; 36 crystals in the 'cross + 45°' and 'ball' setups. The statistical errors are smaller than the data points. Right panel (Colour on-line): A CAD drawing showing thirty six, ø3.8x5.1 cm $LaBr_3$(Ce) crystals coupled to PMTs and housed in aluminium cans in the 'cross+45°' configuration.

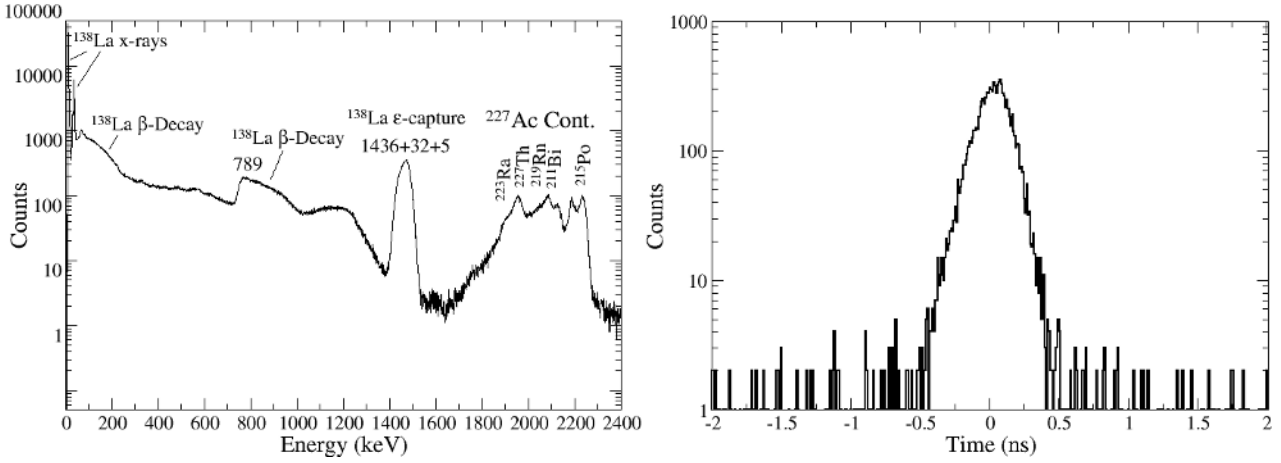

Figure 2. Left panel: A γ-ray spectrum collected over 12 hours showing the self-activity in a ø3.8x5.1 cm $LaBr_3$(Ce) crystal due to contamination from ^{138}La and ^{227}Ac. The peak at 1473 keV is a result of electron capture by ^{138}La, and is shifted by 37 keV due to coincident X-rays. The peaks at energies above ~1.7 MeV correspond to the quenched alpha energies from the decay of ^{227}Ac. Right panel: A TAC spectrum with the thresholds adjusted so that the coincident 1173 and 1332 keV transitions in ^{60}Co correspond to the start and stop channels respectively. Based on this measurement, the intrinsic timing resolution of the ø3.8x5.1 cm detectors was found to be ~210 ps (FWHM).

EasyMCA) after amplification in an ORTEC 572 module. Several calibration sources were used to measure the energy resolution, which was determined to be ~ 3.3 % and ~2.8 % FWHM at energies of 662 and 1332 keV respectively.

The left panel of Figure 2 shows the self-activity in a single $LaBr_3$(Ce) detector due to ^{138}La, a naturally occurring radioisotope with 0.09 % abundance and a half-life of 1.02x10^{11} years. This radioisotope undergoes electron capture (65.6 %) and β^--decay (34.4 %), populating states in ^{138}Ba and ^{138}Ce respectively [17]. There is also contamination from the α-decay of ^{227}Ac, which manifests itself as multiple peaks at energies above 1.7 MeV. Although the α particles have energies in the range of 4-6 MeV, they appear in the 1.7-2.3 MeV [18] range in the γ-ray spectrum due to the quenching of their light signal by 65% [19]. The counting rate for the total self-activity shown in the left panel of Figure 2 was found to be ~5 Hz and ~1 Hz for the ^{138}La and ^{227}Ac contaminants respectively. This is in reasonable agreement with the numbers quoted by Saint-Gobain (~0.7 Hz/cm^3 and ~0.1 Hz/cm^3 for ^{138}La and ^{227}Ac respectively [12]), as each crystal has a volume of ~9 cm^3.

The timing signal was taken from the anode. The 'start' and 'stop' timing signals were sent via a quad CFD (ORTEC 935) to an ORTEC 567 time-to-amplitude converter (TAC), which had a range of 50 ns. An artificial delay of 1.2 ns was added to the 'stop' part of the timing setup. The resulting TAC signal was then sent to an MCA which recorded the signal in 'coincidence-mode'. After calibrating the TAC spectrum, intrinsic timing resolutions of ~210 ps (FWHM) was determined for the coincident 1173 and 1332 keV γ rays from the decay of ^{60}Co, and ~400 ps for coincident 511 keV γ rays in ^{22}Na. These intrinsic timing resolutions have been included in Table 1 and show they are slightly better than the interpolated values. The TAC spectrum of the timing resolution at ^{60}Co energies is shown in the right panel of Figure 2.

4 Conclusions and Outlook

The GEANT4 package was used to carry out Monte-Carlo simulations for a variety of shapes and sizes of $LaBr_3$(Ce) crystals. The timing resolutions of each crystal type were combined with the efficiencies obtained from the GEANT4 simulations to derive an energy-dependent timing precision, resulting in the ø2.5x2.5 cm, ø3.8x3.8 cm and conical crystal types being omitted from further study. As the ø5.1x5.1 cm and ø3.8x5.1 cm crystals had similar precisions, the slightly smaller ø3.8x5.1 cm crystals were preferred over the ø5.1x5.1 cm crystals. Coincidence timing precision calculations were also used to determine the timing resolution a 'hybrid' crystal would need to have in order for a ring to have the same precision as a ring of ø3.8x5.1 cm crystals. For coincident 511 keV γ-rays this was found to be approximately 900 ps.

The two remaining detector types ('hybrid' and ø3.8x5.1 cm cylindrical crystals), were then tiled into different configurations of the full array. Their simulated FEP efficiencies were then compared. The uncertainty in the timing response and energy resolution of the 'hybrid' detectors resulted in the purchase of the ø3.8x5.1 cm cylindrical detectors. These detectors were measured to have an intrinsic energy resolution of 2.8 % (FWHM) at 1332 keV, and an intrinsic timing resolution of ~210 ps (FWHM) for the 'prompt' ($T_{1/2}$=0.9±0.3 ps [20]) 1332 keV, 2^+ level, populated in ^{60}Ni due to the β^--decay from ^{60}Co. Future work will focus on the effect a distributed source of γ-rays from the implantation point will have on the timing precision that can be obtained.

5 Acknowledgments

This project was funded by the UK NuSTAR grant from the Science and Technology Facilities Council (STFC).

References

[1] Green Paper - The Modularized Start Version, http://www.fair-center.eu/fileadmin/fair/publications_FAIR/FAIR_GreenPaper_2009.pdf, October 2009.
[2] H. Geissel et al., Nucl. Instr. Methods B **204**, 71, 2003.
[3] Zs. Podolyák et al., Nucl. Instr. Methods B **266**, 4589, 2008.
[4] P.H. Regan et al., Applied Radiation and Isotopes **70**, 1125, 2012.
[5] N. Mărginean et al., Eur. Phys. J A **46**, 329, 2010.
[6] T. Davinson et al.,http://www2.ph.ed.ac.uk/td/AIDA/Presentations/, 2011.
[7] F.K. Thielman et al., Z. Phys. A **309**, 301, 1983.
[8] A.R. Garcia et al., JINST **7**, 05012, 2012.
[9] D. Rudolph et al., Phys. Rev. C **78**, 021301, 2008.
[10] H. Mach et al., Nucl. Instr. Methods A **280**, 49, 1989.
[11] S. Agostinelli et al., Nucl. Instr. Methods A **506**, 250, 2003.
[12] Saint-Gobain, Scintillation Products Technical Note, BrilLanCe Scintillators Performance Summary, January, 2009.
[13] J.-M. Régis et al., Nucl. Instr. Methods A **622**, 83, 2010.
[14] M. Moszynski et al., Nucl. Instr. Methods A **567**, 31, 2007.
[15] L.M. Fraile et al. ISOLDE Workshop, Fast timing results at ISOLDE, http://indico.cern.ch/getFile.py/access?contribId=36&sessionId=8&resId=0&materialId=slides&confId=67060, November 2009.
[16] H. Mach, priv. comm.
[17] J. McIntyre et al., Nucl. Instr. Methods A **652**, 201, 2011.
[18] F. Quarati et al., Nucl. Instr. Methods A **574**, 115, 2007.
[19] J.K. Hartwell et al., Applied Radiation and Isotopes **63**, 223, 2005.
[20] A. Kluge and W. Thomas, Nucl. Instr. Methods **134**, 525, 1976.